Statistics on Placenta Shapes

Abhishek Bhattacharya

Department of Math, University of Arizona

abhishek@math.arizona.edu

Abstract

In this poster, I present some tools for the statistical analysis of placenta shapes using a random sample of placenta images. This is part of a project carried out by me at Los Alamos National Labs over June-August 2007.

1. Introduction to Placenta shape

THE **placenta** is an organ developed within the uterus of the mother during gestation that is connected to the embryo by the **umbilical cord** and that is discharged shortly after birth. It serves as a structure through which nourishment for the fetus is received from, and wastes are eliminated into, the circulatory system of the mother. Figure 1 shows a placenta specimen.

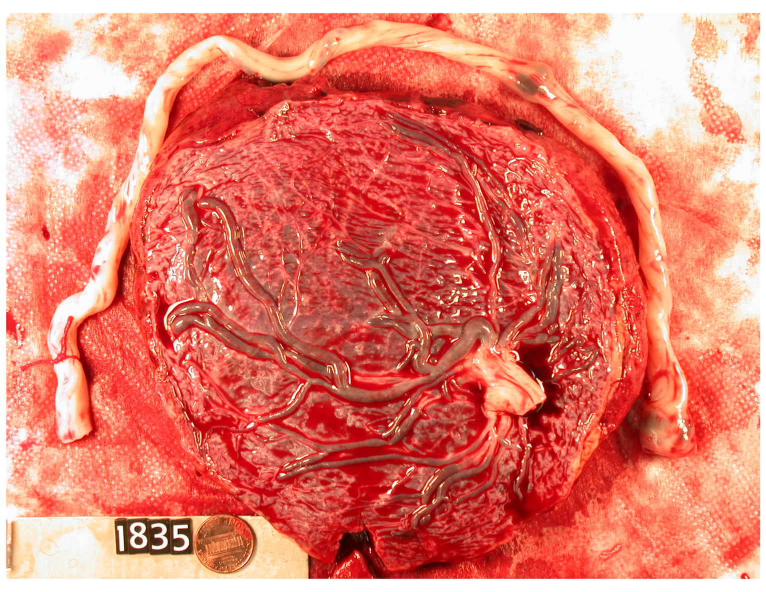

Figure 1: *Placenta 1835 image*

The statistical analysis of placenta shapes based on a random sample of placentas is important in many areas. By noting key features of the shape, like the position of the **Umbilical Cord Insertion point** (CdIns) relative to the outer and inner perimeters, the thickness of the inter perimeter region, shape of the perimeter boundaries (convexity, roundness etc) and others, one may be able to predict features of the new born, like its gender, birth weight, presence of some disease/abnormality etc.

2. Major Findings

IN my project, I compute the mean shape from a random sample of placenta images. I find out that the mean is not circular in shape, unlike what it seems to be (see Figure 6).

I perform a Principal Component Analysis on the tangent space of the mean shape. I notice that perturbaion in shape along different principal directions causes important changes in placenta shape. For example, the CdIns point moves more towards the boundary, the mean loses its convexity etc (see Figure 7).

I study the relation between **Foetal Placental Ratio** (FPR) and placenta shape by

- building a regression model explaining FPR as a function of shape (see Table 2),
- estimating the posterior distribution of FPR given shape, using Kernel based methods.

The regression model explains about 7% of variation in FPR. The posterion distribution of FPR seems to depend a lot on how close or far the shape is from the mean. For shapes closest to the mean, the distribution is the most uniform, while for the most extreme shapes, it is very heterogeneous (see Table 3).

The analyses have been summarized in the subsequent sections.

3. Measuring Placenta shape

TO analyze placenta shapes, we need a mathematical notion of shape. For that, I consider the Kendall's planer shape space Σ_2^k. I pick a set of k points on a 2D placenta image, not all points being the same. We refer to such a set as a **k-ad** or a set of k **landmarks**. Then the **shape** of a k-ad is its orbit or equivalence class under the euclidean motions of translation, rotation and scaling. Σ_2^k is the space of all such orbits or shapes. Thus corresponding to each sample placenta, we get a point on Σ_2^k which represents the placenta shape. Σ_2^k has the structure of the **complex projective space** $\mathbb{C}P^{k-2}$: the space of all complex lines through the origin in $\mathbb{C}^{k-1}$, which is a Riemannian manifold of dimension $2k-4$. Figure 2 shows the chosen k-ad, $k = 41$ for a particular placenta image.

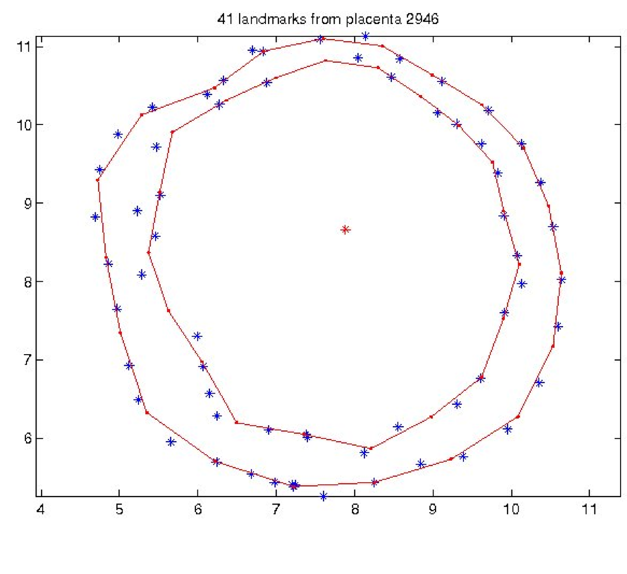

Figure 2: *All landmarks (blue) along with the selected 41 landmarks (red) on Placenta 2946*

The **preshape** of a k-ad is what remains after removing the effects of translation and scaling. It lies on the unit sphere of dimension $2k-3$. Then the planer shape space consists of all one dimensional orbits under rotation of the preshapes. Figure 3a shows 41 landmarks on placentas 1546 and 1528. Figure 3b shows their preshapes. Placenta 1528 preshape has been rotated to bring it closest to the preshape of placenta 1546.

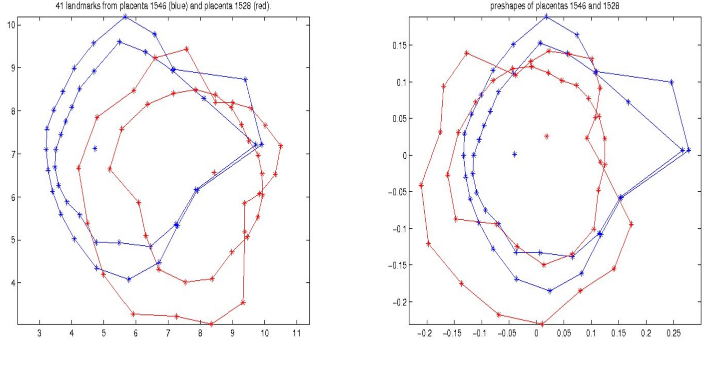

(a) (b)

Figure 3: *(a) 41 landmarks on placentas 1546 (blue) and 1528 (red), (b) Their preshapes*

4. Mean on Manifolds

LET $(\mathbf{M}, \mathbf{g})$ be a d dimensional connected complete Riemannian manifold, g being the Riemannian metric tensor on M. Let ρ be a distance metrizing the topology of M. For a given probability measure Q on M, we define the **Fréchet function** of Q as

$$F(p) = \int_M \rho^2(p, x) Q(dx),\ p \in M. \tag{1}$$

The set of all p for which $F(p)$ is the minimum value of F on M is called the **Fréchet mean set** of Q. If this set is a singleton, say $\{\mu_F\}$, then μ_F is called the **Fréchet mean** of Q. If $X_1, X_2, \ldots, X_n$ are independent and identically distributed (iid) with common distribution Q, and $Q_n \doteq \frac{1}{n}\sum_{j=1}^n \delta_{X_j}$ is the corresponding empirical distribution, then the Fréchet mean set of Q_n is called the **sample Fréchet mean set**, denoted by C_{Q_n}. If this set is a singleton, say $\{\mu_{F_n}\}$, then μ_{F_n} is called the **sample Fréchet mean**.

The natural choice for the distance on M is $\rho = d_g$, the geodesic distance under g. Then the Fréchet mean (set) of Q is called its **intrinsic mean** (set). If $X_1, X_2, \ldots, X_n$ are iid observations from Q, then the sample Fréchet mean (set) is called the **sample intrinsic mean** (set).

In case of the planer shape space Σ_2^k, the projection of a preshape onto its shape is a Riemannian submersion from the unit sphere of dimension $2k-3$ onto Σ_2^k. This makes Σ_2^k a complete Reimannian manifold of dimension $2k-4$. From a result due to Kendall, W.S.(1990), if Q is a probability distribution on Σ_2^k with support in a geodesic ball of radius $\frac{\pi}{4}$, say $B(p, \frac{\pi}{4})$, then it has an intrinsic mean, μ_I, in its support. Also from a result due to Bhattacharya, A. and Bhattacharya, R.(2007), the sample mean from an iid sample has asymptoticaly Normal distribution, if $\mathrm{supp}(Q) \subset B(\mu_I, R)$, where R is the unique solution of $tan(x) = 2x$, $x \in (0, \frac{\pi}{2})$.

Another notion of mean, which is much easier to compute and exists under much broader conditions is called the **extrinsic mean** on manifolds. To get that, we embed M isometrically into some higher dimensional euclidean space via some map, $\Phi : M \to \mathbb{R}^k$. We choose the distance on M as: $\rho(x,y) = \|\Phi(x) - \Phi(y)\|$, where $\|.\|$ denotes Euclidean norm ($\|u\|^2 = \sum_{i=1}^k {u_i}^2$, $u = (u_1, u_2, .., u_k)'$). Let Q be a probability measure on M with finite Fréchet function. The Fréchet mean (set) of Q with respect to the above distance, is called the **extrinsic mean**(set) of Q. If X_j ($j = 1, \ldots, n$) are iid observations from Q, then the sample Fréchet mean(set) is called the **extrinsic sample mean**(set).

In case of $M = \Sigma_2^k$, we embed it into the space $S(k, \mathbb{C})$ of all $k \times k$ complex Hermitian matrices via the **Veronese-Whitney embedding** Φ. $S(k, \mathbb{C})$ is viewed as a (real) vector space of dimension k^2. This gives the **extrinsic distance** ρ on Σ_2^k by that induced from this embedding. Let Q be a probability measure on Σ_2^k, and let $\tilde{\mu}$ denote the mean vector of $\tilde{Q} \doteq Q \circ \Phi^{-1}$, regarded as a probability measure on $\mathbb{C}^{k^2}$ (or, $\mathbb{R}^{2k^2}$). Then it can be shown that the extrinsic mean set of Q is the orbit under rotation of the space of unit eigenvectors for the largest eigen value of $\tilde{\mu}$. It follows that the extrinsic mean μ_E, say, of Q is unique if and only if the eigenspace for the largest eigenvalue of $\tilde{\mu}$ is (complex) one dimensional, and then μ_E is the shape of μ, $\mu (\neq 0) \in$ the eigenspace of the largest eigenvalue of $\tilde{\mu}$. Also it can be shown that in that case, any measurable selection from the sample extrinsic mean set, is a strongly consistent estimator of μ_E, and has asymptotic Normal distribution with mean μ_E.

Using these results, we can construct one and two sample tests to draw inference on the population mean using the sample estimate.

5. Placenta Mean Shapes

GIven a sample of 1101 placenta configurations, I compute the **extrinsic** and **intrinsic** sample mean shapes. These mean shapes can tell a lot about the shape distribution of the random placenta sample.

Figure 4a,b show the preshapes of the extrinsic sample means of 8 inner and outer landmarks respectively along with the corresponding sample landmarks. The sample preshapes have been rotated and scaled so as to minimize their euclidean distances from the mean preshape.

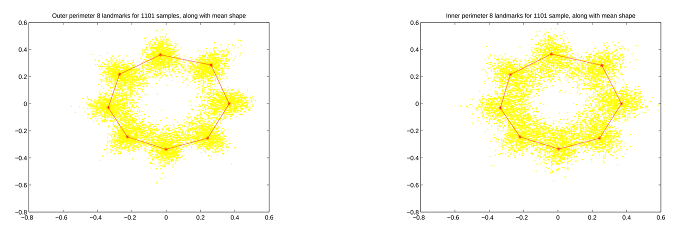

(a) (b)

Figure 4: *(a): 8 landmark outer perimeter mean shape along with sample outer perimeters. (b): 8 landmark inner perimeter mean shape along with sample inner perimeters.*

The figures suggest that both the outer and inner mean shapes are close to being circular, i.e. the 8-ad population mean shapes should be regular octagons. To test that I perform one sample tests, and get p-values of order smaller than 10^{-16}. The very small p-values force me to accept the alternative hypothesis that the sample shapes come from a population whose mean shape is different from a regular octagon. Figure 5 shows the plot of the 2 means along with octagons.

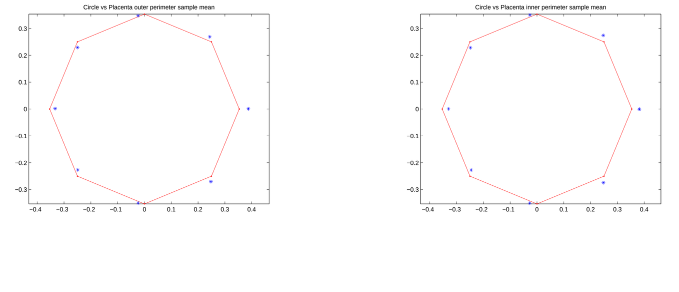

(a) (b)

Figure 5: *(a): 8 landmark outer perimeter mean shape along with a regular octagon. (b): 8 landmark inner perimeter mean shape along with a regular octagon. Red represents octagon edges, blue are the mean shape landmarks*

Figure 6 shows the preshapes of the extrinsic and intrinsic sample means for 41 landmarks. The geodesic distance between the two means is 0.0019. Hence they are almost indistinguishable in the figure. Thus we will get very close results whether we use extrinsic or intrinsic distances in our analysis.

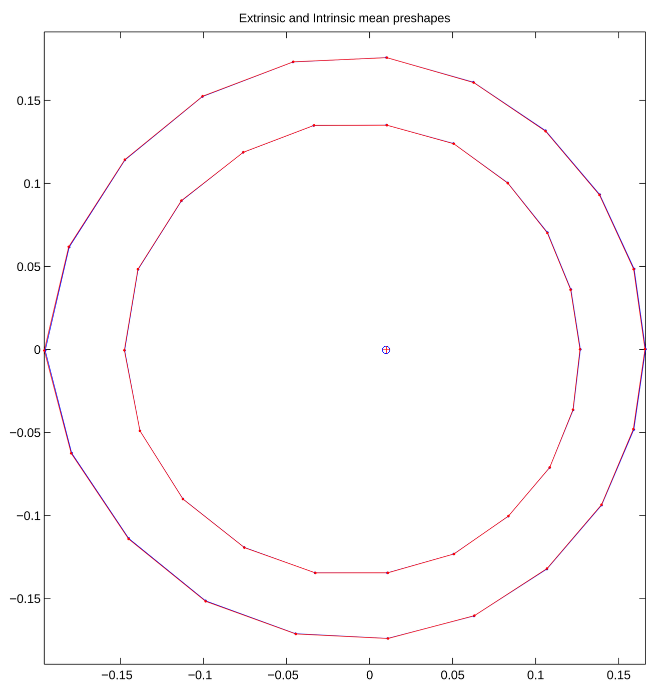

Figure 6: *Blue is the preshape of the extrinsic mean using 41 landmarks, red is the intrinsic mean preshape.*

Having got the intrinsic sample mean shape, I project the data onto the **tangent space** of the planer shape space Σ_2^k, $k = 41$ at the mean using the **inverse exponential map**. That gives $2k-4$ dimensional coordinates for each placenta shape, known as **normal coordinates**. Each placenta shape is a single point in the tangent space and therefore the 1101 sample placentas form a cloud of points in this high dimensional space.

I perform a Principal Component Analysis (PCA) on the cloud of points. Table 1 shows the percent variation and the cumulative percent variation explained by the first 10 principal components(PC). The first two principal components explain about 71% of variation in shape and the first 7 components explain more than 90% of variation in shape. This suggests that placenta shapes lie on a much smaller dimensional submanifold of the shape space, which means that the landmarks are highly correlated.

Table 1: *Percent variation(V) and cumulative percent variation(CV) explained by first few PCs*

PC	1	2	3	4	5	6	7	8	9	10
V	37.8	32.9	7.4	6.7	2.3	2.0	1.7	1.1	0.9	0.9
CV	37.8	70.7	78.1	84.8	87.1	89.0	90.7	91.8	92.8	93.6

What does the distribution of points along the principal directions tell us about placenta shapes? How are placenta shapes affected by movement along principal directions? Figure 7 illustrate the change in the 41-ad intrinsic mean shape caused by perturbations along the first principal direction. The perturbations are measured for times $\pm 1\sigma$ and $\pm 2\sigma$, where $\sigma = \frac{\pi}{18}$ is the standard deviation for the component.

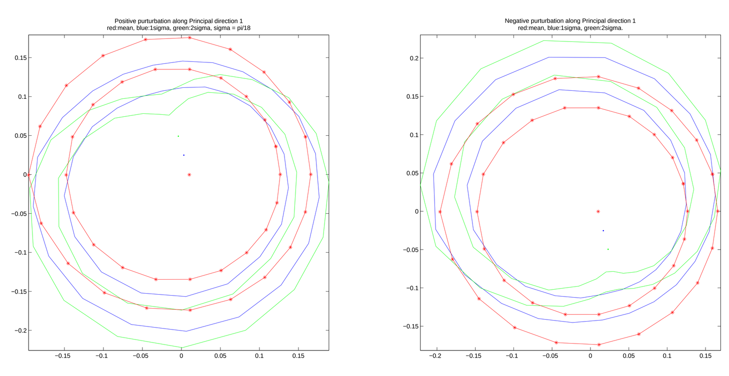

(a) (b)

Figure 7: *(a) Perturbation along Principal direction 1 by 1σ, 2σ from the mean shape. (b) Perturbation by -1σ, -2σ. Red curve is the intrinsic mean of 41 landmarks, blue curves are perturbation by $\pm 1\sigma$, green are $\pm 2\sigma$. $\sigma = \frac{\pi}{18}$*

Figure 7 suggests that perturbation of the mean shape along the first principal direction causes it to lose its convexity and the CdIns point moves more towards the inner perimeter edge.

6. Relation between placenta shape and FPR

THE objective of my project was to study placenta shapes and use them to predict key features of the new born baby, for example, its birth weight, sex, presence of some disease etc. In this section, we study the relation between placenta shape and **Foetal Placental Ratio** (FPR). FPR is the ratio of the birth weight and the placental weight, and hence can be used to get the birth weight of the newborn. Figure 8 shows the scatter plot of geodesic distances of sample shapes from the intrinsic sample mean against the corresponding FPR values. The plot suggests correlation between FPR and placenta shape.

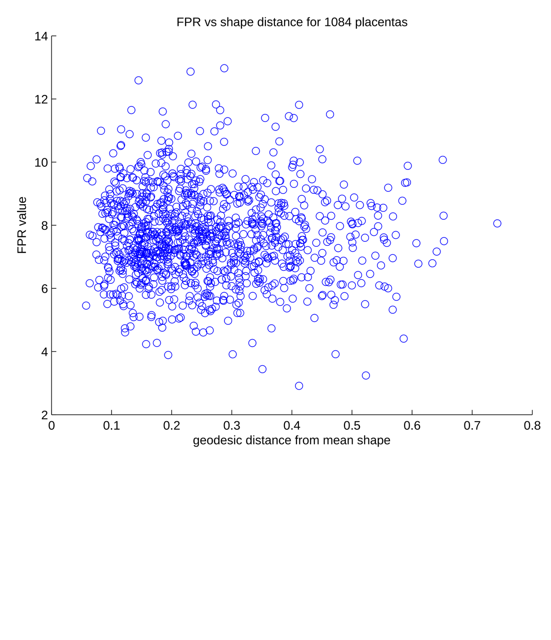

Figure 8: *FPR against placenta shape distance from mean shape*

Figure 9 shows the histogram of the distribution of geodesic distances of sample shapes from the intrinsic mean. The mean distance is 0.2540, and the standard deviation is 0.1201.

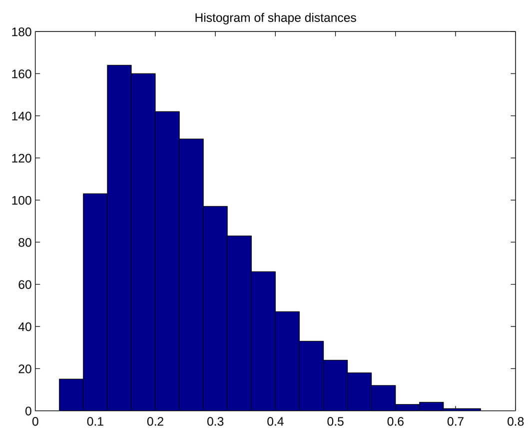

Figure 9: *Histogram of shape distance from mean shape*

To see how the two are correlated, firstly I regress FPR, say y, on the first few principal components of placenta shape, say $\mathbf{x} = (x_1, x_2, \ldots, x_t)$. I try a quadratic model as follows:

$$y = a_0 + \sum_{j=1}^{t} a_j x_j + \sum_{j=1}^{t} b_j x_j^2 + \sum\sum_{1 \le i < j \le t} c_{ij} x_i x_j + \epsilon \qquad (2)$$

For the model (2), I estimate the coefficients, obtain 95% confidence intervals for the coefficients assuming a Normal distribution and use the intervals to test which coefficients are nonzero at level 5%. I also compute the proportion of variation in y explained by the model R^2 and test whether the model has any non zero coefficient other than a_0, i.e. if there is any interaction between y and $\mathbf{x}$. Table 2 shows the results of my analysis. Column 1 shows the shape components used in the model explaining FPR as a function of shape, column 2 lists the estimates of the coefficients in that model that are found to be significant at level 5%, column 3 is R^2 and column 4 is the p-value for the F-test carried out to test for interaction between y and $\mathbf{x}$. If that p-value is less than 5%, I accept the hypothesis that the model has some non zero coefficient other than a_0 and hence is a good model.

Table 2: *Regression of FPR(y) on shape($\mathbf{x}$)*

$\mathbf{x}$	**Significant Coefficients**	R^2	**P-value**
x_1	$\hat{a}_0 = 7.7$, $\hat{a}_1 = -0.64$	0.0069	0.02
(x_1, x_2)	$\hat{a}_0 = 7.75$, $\hat{a}_1 = -0.63$	0.0089	0.0859
(x_1, x_2, x_3, x_4)	$\hat{a}_0 = 7.7$	0.0172	0.1768
$(x_1, x_2, x_3, x_4,)$ $x_5, x_6)$	$\hat{a}_0 = 7.7$, $\hat{a}_5 = 2.6$, $\hat{a}_6 = -2.5$	0.0338	0.1
$(x_1, x_2, x_3, x_4,$ $x_5, x_6, x_7, x_8)$	$\hat{a}_0 = 7.7$, $\hat{a}_5 = 3.24$, $\hat{a}_6 = -3.35$, $\hat{c}_{28} = 25.7$, $\hat{c}_{38} = 43.7$, $\hat{c}_{47} = -25.9$, $\hat{c}_{48} = 33.5$, $\hat{c}_{68} = -65.1$	0.0668	0.004
(x_5, x_6)	$\hat{a}_0 = 7.7$, $\hat{a}_5 = 2.5$	0.0119	0.02

Note that FPR seems to depend on the first principal component (p-value for F-test = 0.02), however adding the second component does not add new information instead just increases the dimension thereby making the model ineffective (p-value for F-test = 0.0859). The table suggests that I should use the model

$$y = a_0 + \sum_{j=1}^{8} a_j x_j + \sum_{j=1}^{8} b_j x_j^2 + \sum\sum_{1 \le i < j \le 8} c_{ij} x_i x_j + \epsilon \qquad (3)$$

This model explains about 6.7% of variation in FPR and the p-value is 0.004 which is fairly small. It is interesting to note that the only non zero linear coefficients are that of principal components 5 and 6 and there are no non zero quadratic terms. This suggests that FPR depends on shape linearly through components 5 and 6. Of course there are non zero interaction terms like the coefficients of $x_2x_8, x_3x_8, x_4x_7, x_4x_8$ and x_6x_8. Figure 10 shows FPR as a quadratic function of principal components 5 and 6. This model explains 1.19% of FPR variation.

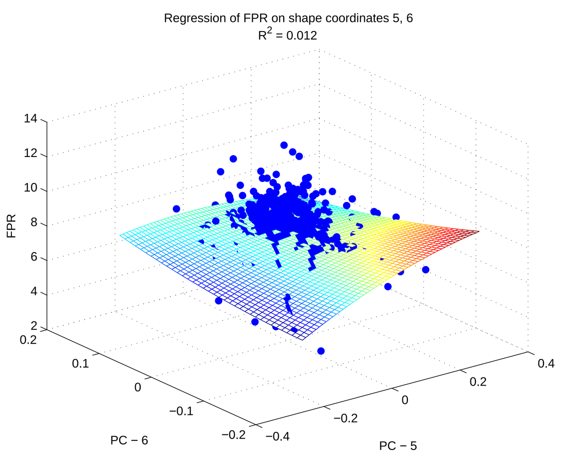

Figure 10: *Scatter plot of FPR against x_5, x_6 along with best quadratic model*

Next I use nonparametric density estimation on manifolds, to estimate the posterior distribution of FPR (y) given the placenta shape. To do that, I divide the FPR values into 5 ordered classes, say, $(-\infty, a_1]$, $(a_1, a_2]$, $(a_2, a_3]$, $(a_3, a_4]$ and (a_4, ∞) and then estimate the probability that considering the placenta shape alone, the placenta will fall into a particular FPR class.

To get the partition points dividing the FPR classes, $a_1, \ldots, a_p$, $p = 4$, I maximize the weighted sum of squared distances between the means of the $p+1$ groups, or equivalently, minimize the weighted sum of within group variations. The weights are proportional to the probability of the groups. Mathematically, I choose $\mathbf{a} = (a_1, \ldots, a_p)$, $p = 4$ so as to maximize

$$\phi(\mathbf{a}) = \sum_{i=1}^{p+1} P(a_{i-1}, a_i] \left(\mathrm{E}(Y|a_{i-1} < Y \le a_i) - \mathrm{E}(Y)\right)^2 \qquad (4)$$

with respect to $\mathbf{a}$. In (4), P denotes the FPR probability distribution and Y has distribution P. There $a_0 = -\infty$ and $a_{p+1} = \infty$. Given an iid sample $Y_1, \ldots, Y_n$ with common distribution P, I get sample estimate for $\mathbf{a}$, $\hat{\mathbf{a}} = (\hat{a}_1, \ldots, \hat{a}_p)$ by replacing P in (4) by the sample empirical distribution, P_n. For this specific sample,

$$\hat{a}_1 = 5.985,\ \hat{a}_2 = 7.245, \hat{a}_3 = 8.354,\ \hat{a}_4 = 9.71.$$

Figure 11 shows the histogram of the FPR values along with the 5 classes. Red lines denote class boundary. Note that there are other ways of classifying FPR values, for example that can be done based on some biological consideration, but for this case, I use purely statistical reasoning.

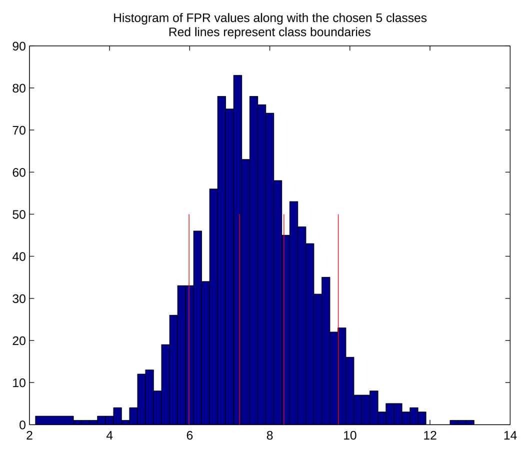

Figure 11: *Histogram of FPR values classified into 5 classes*

If the prior probabilities of the $p+1$ classes are $\pi = (\pi_1, \ldots, \pi_{p+1})$ ($\pi_j = P(a_{j-1}, a_j]$, $j = 1, \ldots, p+1$), then their posterior probabilities given a shape $\mathbf{x}$ are $\varpi(\mathbf{x}) = (\varpi_1(\mathbf{x}), \ldots, \varpi_{p+1}(\mathbf{x}))$ where

$$\varpi_j(\mathbf{x}) = \frac{f(\mathbf{x}|Y \in (a_{j-1}, a_j])\pi_j}{\sum_{j=1}^{p+1} f(\mathbf{x}|Y \in (a_{j-1}, a_j])\pi_j},\ j = 1, \ldots, p+1. \qquad (5)$$

Here $f(\mathbf{x}|Y \in (a_{j-1}, a_j])$ represents the conditional shape density for the class $Y^{-1}(a_{j-1}, a_j]$. We estimate that by the Kernel density estimate,

$$\hat{f}_{\sigma j}(\mathbf{x}) = \frac{1}{n_j} \sum_{j: Y_j \in (\hat{a}_{j-1}, \hat{a}_j]} \frac{e^{-\frac{1}{2}\frac{d_g^2(X_j, \mathbf{x})}{\sigma^2}}}{\int_{\Sigma_2^{41}} e^{-\frac{1}{2}\frac{d_g^2(y, \mathbf{x})}{\sigma^2}} V(dy)},\ j = 1, \ldots, p+1 \qquad (6)$$

for appropriately chosen σ. Here $X_1, \ldots, X_n$ is the iid shape sample and n_j is the the number of shapes in the class $C_j = \{X_i : Y_i \in (\hat{a}_{j-1}, \hat{a}_j]\}$. Then we estimate the posterior probability, $\varpi_j(\mathbf{x})$ by

$$\hat{\varpi}_j(\mathbf{x}) = \frac{\hat{f}_{\sigma j}(\mathbf{x})\hat{\pi}_j}{\sum_{j=1}^{p+1} \hat{f}_{\sigma j}(\mathbf{x})\hat{\pi}_j},\ j = 1, \ldots, p+1. \qquad (7)$$

Here $\hat{\pi}_j$ is the proportion of Y_j's in $(\hat{a}_{j-1}, \hat{a}_j]$. For our sample, they are

$$\hat{\pi}_1 = 0.11,\ \hat{\pi}_2 = 0.30, \hat{\pi}_3 = 0.31,\ \hat{\pi}_4 = 0.21,\ \hat{\pi}_5 = 0.07.$$

Table 3 shows the posterior probabilities $\hat{\varpi}_j$, $j = 1, 2, \ldots, 5$ for a few shapes when I take $\sigma = 0.07$.

Table 3: *Posterior probabilities ($\hat{\varpi}$) for a few placentas*

Placenta Id	**Geodesic Distance from mean shape**	$\hat{\varpi}_1$	$\hat{\varpi}_2$	$\hat{\varpi}_3$	$\hat{\varpi}_4$	$\hat{\varpi}_5$
2946	0.0577	0.1015	0.2887	0.3239	0.2216	0.0642
2163	0.0596	0.0960	0.2983	0.3257	0.2166	0.0634
2919	0.0636	0.1061	0.2878	0.3202	0.2214	0.0645
2639	0.0637	0.0966	0.2974	0.3265	0.2139	0.0657
2830	0.0653	0.0869	0.3062	0.3125	0.2319	0.0625
3363	0.0678	0.0891	0.3020	0.3281	0.2189	0.0619
2561	0.0682	0.1059	0.2973	0.3259	0.2131	0.0578
3062	0.0746	0.0973	0.2989	0.3140	0.2116	0.0782
2645	0.0750	0.0966	0.3107	0.3203	0.2140	0.0584
2957	0.0750	0.0954	0.3036	0.3185	0.2088	0.0737
3303	0.2300	0.1469	0.2413	0.3114	0.1747	0.1257
2630	0.2306	0.1006	0.2788	0.3117	0.2288	0.0801
2620	0.2308	0.1268	0.4238	0.2330	0.1767	0.0397
2007	0.2309	0.0655	0.3128	0.2580	0.2772	0.0865
3396	0.2314	0.1476	0.2720	0.2931	0.1640	0.1233
2938	0.2318	0.4820	0.1625	0.1839	0.1035	0.0681
1730	0.2321	0.1166	0.3423	0.2932	0.1660	0.0818
2788	0.2321	0.0714	0.4759	0.1959	0.2054	0.0515
2648	0.2325	0.0302	0.1373	0.1312	0.6827	0.0186
2126	0.2326	0.1119	0.3083	0.2540	0.2491	0.0765
2732	0.5915	0.0001	0.9423	0.0462	0.0011	0.0103
1976	0.5929	0.0000	0.9993	0.0000	0.0006	0.0000
1762	0.6073	0.0000	1.0000	0.0000	0.0000	0.0000
1832	0.6105	0.0000	0.0155	0.0053	0.0019	0.9773
2776	0.6338	0.0148	0.9807	0.0004	0.0002	0.0040
1806	0.6410	0.0000	1.0000	0.0000	0.0000	0.0000
3244	0.6510	1.0000	0.0000	0.0000	0.0000	0.0000
2107	0.6525	0.0000	0.0014	0.0187	0.9798	0.0001
3061	0.6531	0.0000	0.0006	0.0035	0.0115	0.9844
1921	0.7419	0.0000	0.0000	0.0000	0.9999	0.0000

The first 10 placentas in the table are the ones with shapes closest to the (intrinsic) mean shape. The next 10 are the ones with shape distance in the middle, and the last 10 have shapes furthest from the mean. Note how the FPR distribution changes for the 3 shape groups. The first group placenta shapes seem to have the most homogeneous conditional FPR distribution, while for the last 10, the distribution seems to be the least homogeneous. In the table, Placenta 1806 with shape distance 0.64 belongs to class 2 , i.e. the one with FPR in (6.0, 7.2], with probability 1. That seems to be consistent with Figure 8 because placenta 1806 has an FPR value of 7.17. However placenta 3244 with shape distance 0.65 belongs to class 1, i.e. has FPR less than 6 with probability 1 which does not seem to be consistent with Figure 8, because this placenta has a FPR of 10.07 (class 5). This discrepency may be justified, if we note that our probability estimates depend on the entire shape and not just on the shape distance from the mean.

Future work

We can get many interesting results by analyzing placenta shapes in more detail.

If I continue this project in future, I may carry out two sample tests to discriminate between placenta shapes of opposite sexes. Also I may carry out the regression of FPR on shape separately for the two sex and may get very different results. This regression can be done nonparametrically, rather than assuming a quadratic model. In such a model, I estimate the posterior mean of FPR given placenta shape using kernel based methods.

Another important analysis will be to use placenta size and shape information to predict new born features. A measure of placenta size can be the placenta weight. Using size and shape information together, we may get much stronger models explaining FPR.

To get more information on shape, I may consider the shape of 3-D configurations from the whole placentas. That requires statistical analysis tools on a different manifold, namely Σ_3^k, and some methodologies have been developed in recent times.

Finally, to measure placenta shape more accurately, I may also include the position of the blood vessels, nerve endings etc in the shape. These features can tell us a lot about the new born.